

Optimization of Anchor Structure for MEMS Comb Driven Acoustic Emission Transducers Based on the Principles of Area and Gap Changes

Ning Su*

School of Physics and Electronic Engineering, Jiangsu University, 212013, Zhenjiang, China

*Email: sn1150610019@gmail.com

Abstract: The focus of this article is to provide an optimized design scheme for the anchor structure of the comb capacitive acoustic emission sensor to enhance its response ability. Firstly, variable area and variable spacing sensing microelements were designed, and their basic performance parameters were obtained through finite element analysis. Using the peak response changes corresponding to the first order characteristic frequency as a reference standard, the influence of the geometric structure of the anchor section on the response was analyzed.

Keywords: Acoustic emission, Comb structure, MEMS, Anchor loss.

1. Introduction

Structures or materials are prone to damage during manufacture and use, and along with the damage, molecular bonds are broken and stress waves are generated [1], which can also be referred to as acoustic emission signals in acoustic emission techniques. Acoustic emission technology is an important detection method in NDT by receiving and analyzing acoustic emission signals to determine the onset of damage generation, locate the location of damage, and assess the extent of damage [2,3].

Acoustic emission sensors are the core of acoustic emission technology and can be mainly classified into resonant (narrow-band type) or wide-band type according to the response frequency domain, and into traditional block-type acoustic emission sensors and MEMS acoustic emission sensors according to the volume. Because of the small size and low sensitivity of MEMS acoustic emission sensors compared with traditional sensors, MEMS acoustic emission sensors are generally designed as resonant type to improve their sensitivity and signal-to-noise ratio [4].

The main limitation of resonant MEMS acoustic emission sensors is the loss of mechanical energy, when the acoustic emission signal propagates from the sensor base to the resonant structure of the sensor there is a dissipation of energy, the degree of energy dissipation is measured by the quality factor Q [5], the quality factor is affected by a variety of circumstances, including air damping, anchor loss, etc [6]. Air damping can be solved by designing structures to reduce air damping [7,8] or by evacuating [9], while reducing anchor losses is mainly achieved by designing new anchor structures. For example, Ardito et al [10] formed a phonon crystal structure by fabricating a series of column arrays on the anchor to confine the wave signal in the resonant structure, which is a practical novel design for structures manufactured by surface silicon technology with low thickness requirements. Zou [11] et al designed a butterfly-shaped aluminum nitride (AlN) plate structure for Lamb wave resonators, using a butterfly-shaped topology to effectively change the displacement field of the AlN plate, increasing the Q value from 3360 to 4758. Novel designs such as these are

based on surface silicon technology for sensing structures. Capacitive acoustic emission sensors, whose performance does not depend on the properties of the manufacturing material, depend mainly on the design of the structure itself. The anchor body of the resonant structure becomes larger.

In conventional designs, the anchor body is often designed as a rectangular structure, but the exact size of the rectangular structure has not been fully investigated. In this paper, two comb-tooth capacitive sensing microelements with different capacitance change mechanisms (gap-change type and area-change type) and better performance are designed using finite element simulation analysis, and the effect of the anchor body cross-section parameters on the response characteristics of the sensing microelements is investigated as measured by their displacement response cases to provide an optimized solution for the structural design of comb-tooth capacitive acoustic emission sensing microelements manufactured by the body-silicon process.

This study is organized as follows: in Section I, the acoustoelectric conversion mechanism of two types of comb-tooth structures is given; in Section II, the design parameters of the sensing microelement are given, and the first three orders of eigenmodes as well as the frequency domain displacement response are determined by finite element analysis; in Section III, the effect of the anchor body cross-section parameters on the peak displacement response of the sensing microelement is revealed, and then an optimization method to reduce the anchor loss of the sensing microelement with comb-tooth structure is proposed; in Section III, the effect of the anchor body cross-section parameters on the peak displacement response of the sensing microelement is revealed; Section IV summarizes this work and presents the shortcomings and outlook.

2. Working Principle of Comb Type Acoustic Emission Sensor

The acoustic emission sensing structure sensitive to in-plane signals mainly consists of a fixed electrode containing a comb, an anchor body and a resonant structure consisting of a mass block containing a comb and a micro spring, as shown in Figure 1. The anchor body, fixed electrode and its fixed

comb teeth are directly attached to the surface of the substrate, and the mass block and micro spring are connected to the anchor body at both ends and left with a certain gap with the substrate. As shown in Figure 1(a), the direction of deformation of the microspring susceptibility of the area-change acoustic emission sensing micro-element is the same

as the change in the squared area of the comb capacitance, and in Figure 1(b), the direction of deformation of the microspring susceptibility of the gap-change acoustic emission sensing micro-element is the same as the change in the pitch of the comb capacitance.

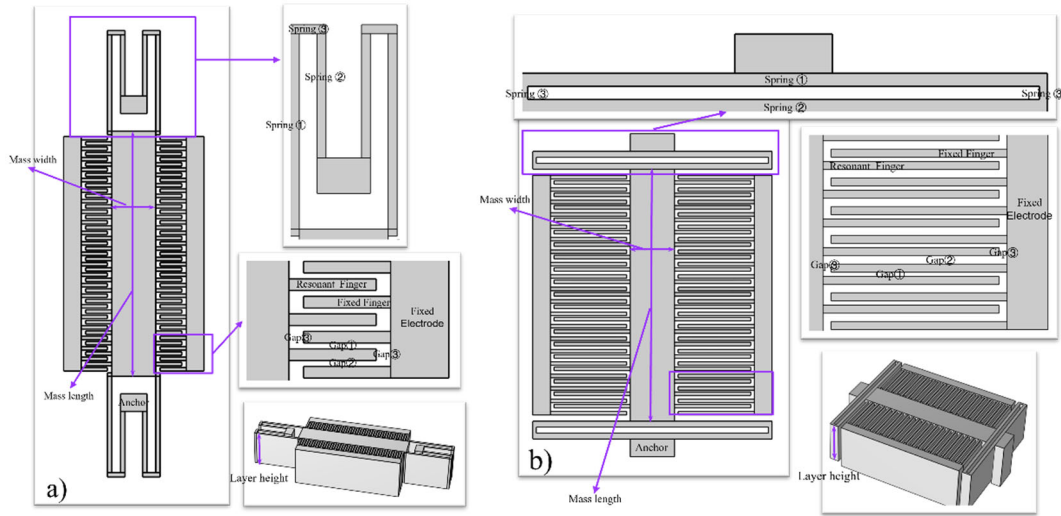


Figure 1. Basic structure of capacitive in-plane acoustic emission sensing micro-element: (a) Area-change acoustic emission sensing micro element; (b) Gap-change acoustic emission sensing micro element

One of the simplified models of the area-change acoustic emission sensing micro-element is shown in Figure 2. In its

operating state, the change of comb capacitance on both sides of its mass block is reversed, so both sides need to be analyzed.

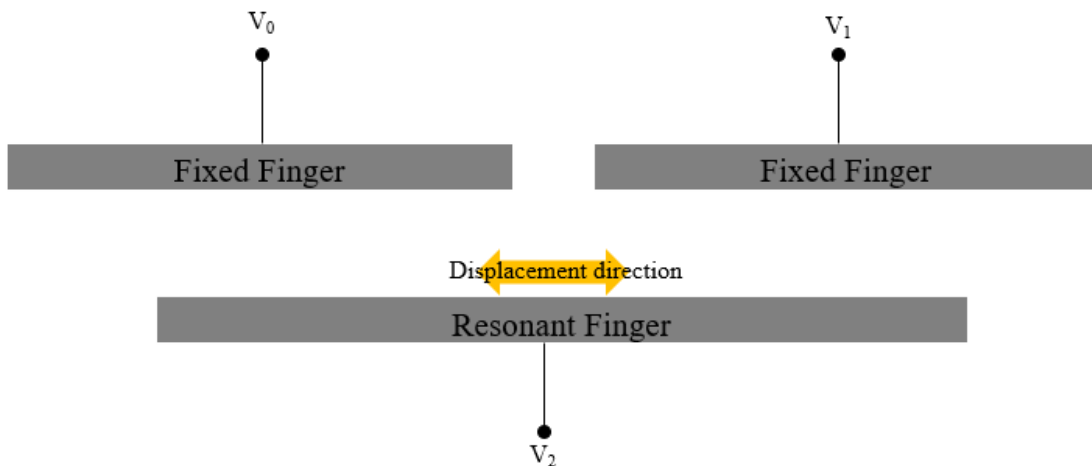


Figure 2. Electrical analysis model of Area-change acoustic emission sensing micro-element

When it is excited by the signal resulting in a displacement of x in the direction of the resonant spacing along the area change at time t , its average output current can be expressed by equation 1 as :

$$i = \frac{dQ}{dt} = (V_0 - V_2) \frac{dC_0}{dt} + (V_1 - V_2) \frac{dC_1}{dt} = (V_0 - V_2) \frac{\epsilon h}{d} \frac{dx}{dt} - (V_1 - V_2) \frac{\epsilon h}{d} \frac{dx}{dt} \quad (1)$$

Where h is the height of the resonant comb and dx/dt is the change in displacement of the comb in the direction of area

change. According to Eq. 1, in the design of the area-change acoustic emission sensing micro-element, the fixed electrodes on both sides need to be connected to different potentials and the resonant structure needs to be connected to a potential between the two to generate a larger current.

For the gap-change sensing micro-element, the change in capacitance of the combs on both sides of its mass block in the operating condition is the same, so one side can be analyzed separately. For one resonant comb, the capacitance structure can be formed separately from the two adjacent fixed combs, as shown in Figure 3.

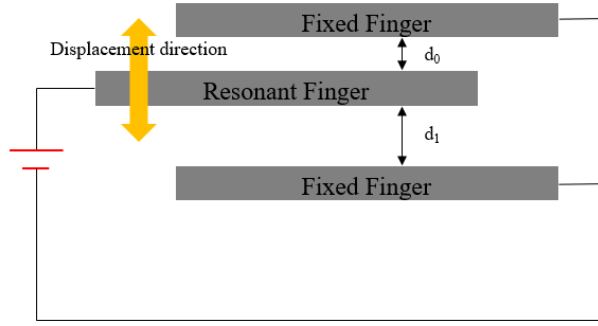


Figure 3. Electrical analysis model of Gap-change acoustic emission sensing micro-element

When it is subjected to signal excitation resulting in a change in comb pitch at time t , the average output current can be expressed by Equation 2 as:

$$i = \frac{dQ}{dt} = V_{DC} \frac{dC}{dt} = V_{DC} \left(\frac{\epsilon S}{d_0 - d} - \frac{\epsilon S}{d_1 + d} \right) \quad (2)$$

Where V_{DC} is the DC bias added between the resonant structure and the fixed comb, and S is the square area between the combs. According to Eq. 2, it can be seen that the fixed electrodes on both sides can be kept at the same potential during the design of the gap-change acoustic emission sensing

micro-element, and d_0 and d_1 need to be deliberately designed to have a certain gap value to avoid serious current cancellation.

3. Structural Design and Finite Element Analysis

3.1. Structural design

The structural and material parameters of the sensing microelements are shown in Table 4.

Table 4. Combination parameters and material parameters of area-change and gap-change acoustic emission sensing microelements

Type	Geometries (length×width×height) dimensions in (μm)						Gaps(μm)		
	Mass	Finger	Spring①	Spring②	Spring③	Anchor	Gap①	Gap②	Gap③
Area-Change	280*50*90	30*4*90	5*114*90	5*70*90	20*5*90	30*20*100	2	2	5
Gap-Change	284*50*90	86*4*90	270*6.6*90	270*6.6*90	4*6.8*90	20*50*100	2	4	4
Young's modulus		Relative dielectric constant		Density			Poisson's ratio		
158GPa		45		2320kg/m ³			0.22		

3.2. Finite element analysis

3.2.1. Characteristic frequency analysis

The first three orders of eigenmodes and frequencies of the

area-change and gap-change acoustic emission sensing microelements are shown in Fig. 5.

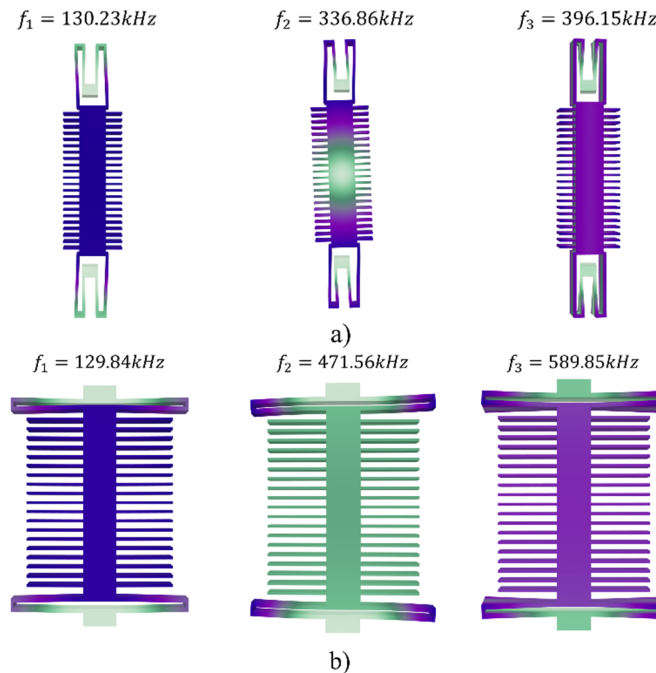


Figure 5. The first three orders of eigenfrequencies and modes of each sensing micro-element. a) area-change ;b) gap-change

According to the eigenfrequency analysis, it can be seen that the frequencies corresponding to the higher-order modes of the microelements designed in this paper are much larger than the fundamental frequencies, implying that the sensing microelements can effectively distinguish the modes.

3.2.2. Frequency domain displacement response

In the simulation model shown in Figure 6, the resonant

structure of the sensing micro-element is placed on a solid plate with similar dimensions to the inter-micro-element, and a displacement in the specified direction is applied to the plate to simulate the displacement of the acoustic emission signal propagating to the substrate near the micro-element.

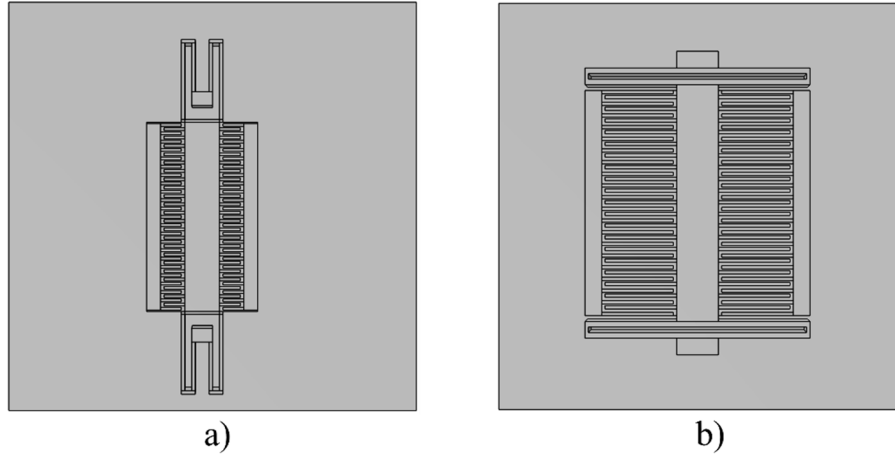


Figure 6. Simulation model structure. a) area-change; b) gap-change type

Simulated acoustic emission signals in the direction of area change/spacing change are applied to the two plates separately with an amplitude of $0.01 \mu\text{m}$ and a frequency

range of 50-500 kHz, and the corresponding displacement response is shown in Figure 7.

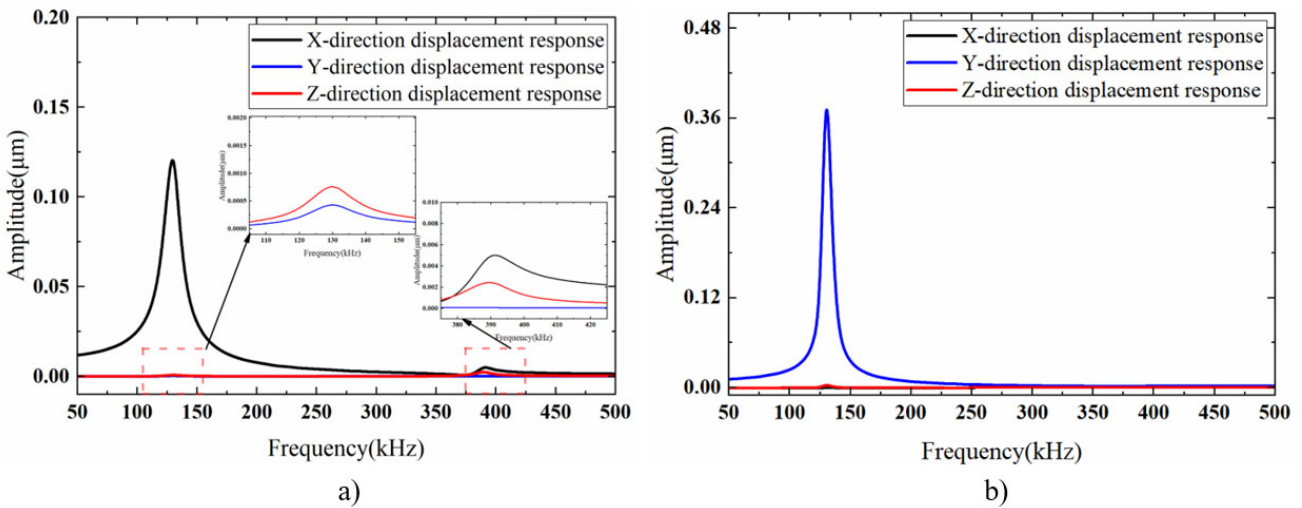


Figure 7. Displacement response. a) area-change; b) gap-change type

From the displacement response, it can be seen that the sensing micro-element designed in this paper has a single fundamental frequency mode vibration behavior and can respond to the acoustic emission signal more accurately.

4. Anchor Optimization Analysis

Since the sensing structure is designed as a structure with a certain height, it is not suitable to optimize the height of the anchor, so only the cross-sectional parameters of the anchor

will be optimized.

4.1. Gap-change anchor analysis

For gap change sensing micro elements, once the parameters of their resonant structure are determined, the width of the anchor tightly connected to the micro spring cannot be changed. Therefore, for gap change sensing micro elements, only the influence of anchor length on gap change is discussed. Analyze its peak displacement response. As shown in Figure 8.

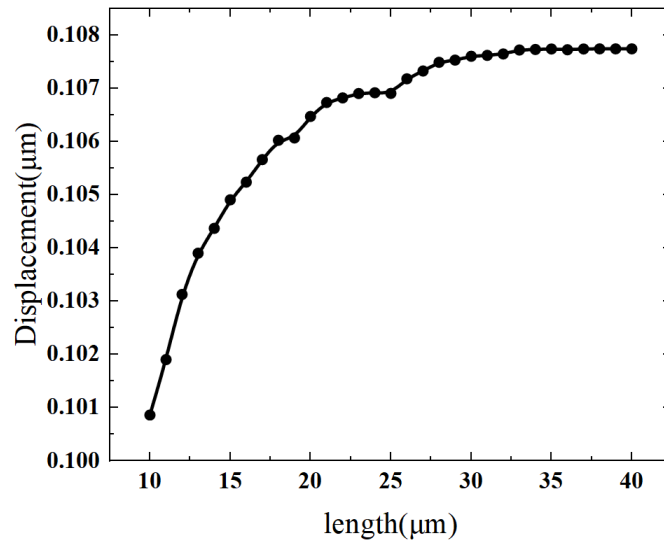


Figure 8. The influence of gap-change anchor length on the peak displacement response

From Figure 8, it can be seen that increasing the anchor length can enhance the displacement response of the resonant structure to a certain extent, but the optimization effect tends to be smooth when the length reaches a certain value.

4.2. Gap-change anchor analysis

For the area-change structure, anchor section has greater optimization space, so the peak displacement response for different aspect ratio sections is shown in Figure 9.

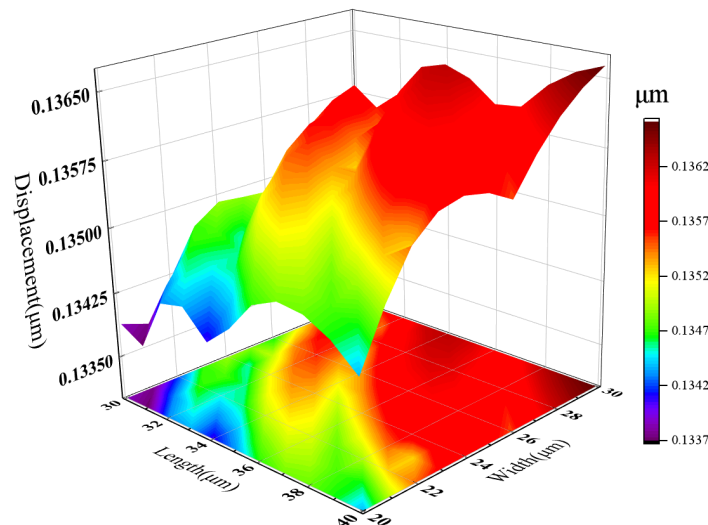


Figure 9. The influence of gap-change anchor length and width on the peak displacement response

It can be seen from Figure 9 that, firstly, unilaterally increasing the length or width is beneficial to the enhancement of the resonant displacement response, and secondly, according to the trend of the three-dimensional graph, it can be seen that increasing the anchor width is more beneficial to the enhancement of the resonant displacement response.

In summary, making the anchor somewhat longer in the plane orthogonal to the sensitive direction of the sensing micro-element is conducive to improving the response of the sensing micro-element.

5. Conclusion

In this study, area-change and gap-change acoustic emission sensing microelements are designed and the better performance of the design is determined by finite element

simulation. The analysis focuses on the displacement response of the resonant structure with respect to the anchor cross-section parameters in the above model. The results show that for the gap-change acoustic emission sensing micro-element, the response displacement of the resonant structure increases with the increase of the anchor section length and then stabilizes; for the area-change sensing micro-element, increasing the length and width of the anchor section can improve the response displacement to a certain extent, but increasing the anchor section width is a more effective way to optimize the response displacement.

References

- [1] Kral Z, Horn W, Steck J. Crack propagation analysis using acoustic emission sensors for structural health monitoring systems. *ScientificWorldJournal*. 2013 Aug 20;2013:823603.

- doi: 10.1155/2013/823603. PMID: 24023536; PMCID: PMC3760098.
- [2] Schumacher, Thomas; Higgins, Christopher C.; Lovejoy, Steven C.. Acoustic emission monitoring of conventionally reinforced concrete highway bridges under service conditions[J]. RILEM Bookseries, 2012, Vol.6: 847-852.
- [3] Leone Jr., F.A.; Ozevin, D.; Awerbuch, J.; Tan, T.-M.. Detecting and locating damage initiation and progression in full-scale sandwich composite fuselage panels using acoustic emission (Article) [J]. Journal of Composite Materials, 2013, Vol.47(13): 1643-1664.
- [4] Ozevin D . MEMS Acoustic Emission Sensors[J]. Applied Sciences, 2020, 10(24):8966.
- [5] Aimi A , Desiderio L , Fedeli P , et al. A fast boundary-finite element approach for estimating anchor losses in Micro-Electro-Mechanical System resonators [J]. Applied Mathematical Modelling, 2021, 97:-.
- [6] Luiz, G.O.; Benevides, R.S.; Santos, F.G.S.; Espinel, Y.A.V.; Mayer Alegre, T.P.; Wiederhecker, G.S.. Efficient anchor loss suppression in coupled near-field optomechanical resonators[J]. OPTICS EXPRESS, 2017, Vol.25(25): 31347-31361.
- [7] Harris, A.W., Oppenheim, I.J., Greve, D.W.. MEMS-based high-frequency vibration sensors [J] Smart Materials & Structures. 2011.20(7):075018-1-075018-9.
- [8] Saboonchi, Hossain, Kabir, et al. MEMS sensor fusion: Acoustic emission and strain[J]. Sensors and Actuators, A. Physical, 2016.
- [9] Wright A P , Wei W U , Oppenheim I J , et al. DAMPING, NOISE, AND IN-PLANE RESPONSE OF MEMS ACOUSTIC EMISSION SENSORS[J]. Journal of Acoustic Emission, 2007, 25:p.115-123.
- [10] J. Zou, C. -M. Lin and A. P. Pisano, "Quality factor enhancement in Lamb wave resonators utilizing butterfly-shaped AlN plates," 2014 IEEE International Ultrasonics Symposium, Chicago, IL, USA, 2014, pp. 81-84, doi: 10.1109/ULTSYM.2014.0021.